A HIGH DEFINITION MAP ASSISTED POTHOLE DETECTION METHOD FOR MOBILE LASER SYSTEM

Yun-Chen Tiao [1] and Chi-Kuei Wang [2]
[1] Dept. of Geomatics, National Cheng Kung University, No. 1, Daxue Rd., East Dist., Tainan 70101, Taiwan (R.O.C.),
Email: tiao980404@gmail.com
[2] Dept. of Geomatics, National Cheng Kung University, No. 1, Daxue Rd., East Dist., Tainan 70101, Taiwan (R.O.C.),
Email: chikuei@mail.ncku.edu.tw

KEY WORDS: Pothole detection, Mobile LiDAR Systems, Point cloud data

ABSTRACT: Road pavement is often damaged due to traffic load, weather and other factors. Therefore, periodic inspection and maintenance are required. Among the many types of road pavement distresses, potholes are particularly significant and can cause serious traffic accidents. The traditional pothole detection method requires inspectors to visit the site to measure, which is labor-intensive and dangerous. Nowadays, mobile laser system (MLS), which has been widely used recently with the advancement of technology, is used in this study to collect detailed 3D information of the road surface. To reconstruct the three-dimensional scene, this study uses NDT matching to match the MLS point cloud with high definition map (HD map) as the base map. Pothole detection is performed on the road pavement in the 3D point cloud scene using the best-fitting plane algorithm and the sightline blocked azimuth ratio algorithm.

1. INTRODUCTION

In the national infrastructure construction, road pavement is an important project. Road pavement will be damaged due to traffic load, weather conditions and the surrounding environment, which will affect driving safety. The damage of potholes is particularly serious, and the appearance of potholes may cause vehicle tires to explode and riders to fall at high speed, resulting in serious traffic accidents. Therefore, the government needs to regularly detect and carry out maintenance operations. However, the traditional measurement method requires inspectors to measure the size and depth of the pothole in person, which is labor-intensive and dangerous. To improve efficiency, we try to use instruments to assist inspection operations and reduce the number of inspectors every time they go out. In recent years, the development of mobile laser systems (MLS) has gradually matured, and a large-scale 3D point cloud can be obtained to obtain road pavement information. De Blasiis et al. propose a method that uses the best fitting plane to calculate the difference in elevation for each point cloud to identify pavement potholes and swells. Ravi et al. also used the best fitting plane to detect potholes. Before the calculation of the best fitting plane, the road surface was cut into road tiles, and the plane was fitted in units of road tiles to reduce the amount of calculation and speed up the calculation.

In this paper, the point cloud data is obtained by the mobile laser system. The 3D point cloud scene is reconstructed by NDT matching through the point cloud base map of the high-definition map. Pavement pothole is detected using the best fitting plane algorithm and the sightline blocked azimuth ratio algorithm.

2. TEST DATA

This experiment uses a self-built mobile laser system. Figure 1 shows the hardware equipment used in this experiment. A lidar (HDL-64E) is installed on the roof of the vehicle (PEUGEOT 3008). HDL-64E is a LiDAR with 64 beams scanning at the same time. The horizontal scanning range is 360 degrees and the vertical scanning range is 26.8 degrees, including 2 degrees horizontally upward and 24.8 degrees horizontally downward. The measuring distance can reach 120 meters.

Figure 1. Mobile laser system a. PEUGEOT 3008 b. HDL-64E

In this experiment, from December 2021 to January 2022, 30 experimental sites were obtained in Tainan City, Taiwan, with a total of 41 potholes. The vehicle speed was about 20 km/hr, and the point density was 3000 points/m^2. The location of the experimental area as shown in Figure 2.

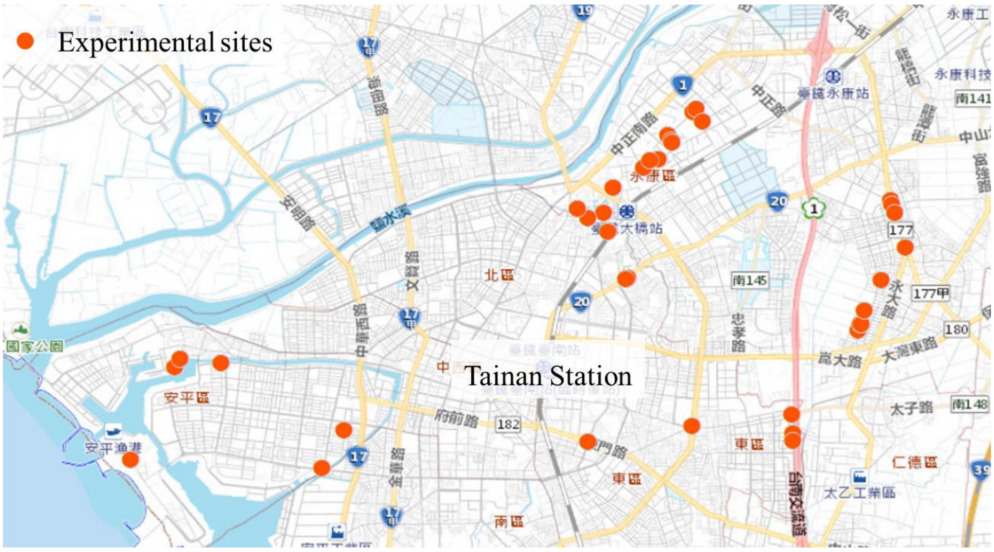

Figure 2. Experimental sites

3. METHODOLOGY

In the existing related literature, most of the pothole positions are calculated by the best fitting plane algorithm, which can effectively calculate the depression in the local area. Based on the best fitting plane algorithm, this study adds the sightline blocked azimuth ratio algorithm for road pothole detection. The process is shown in Figure 3.

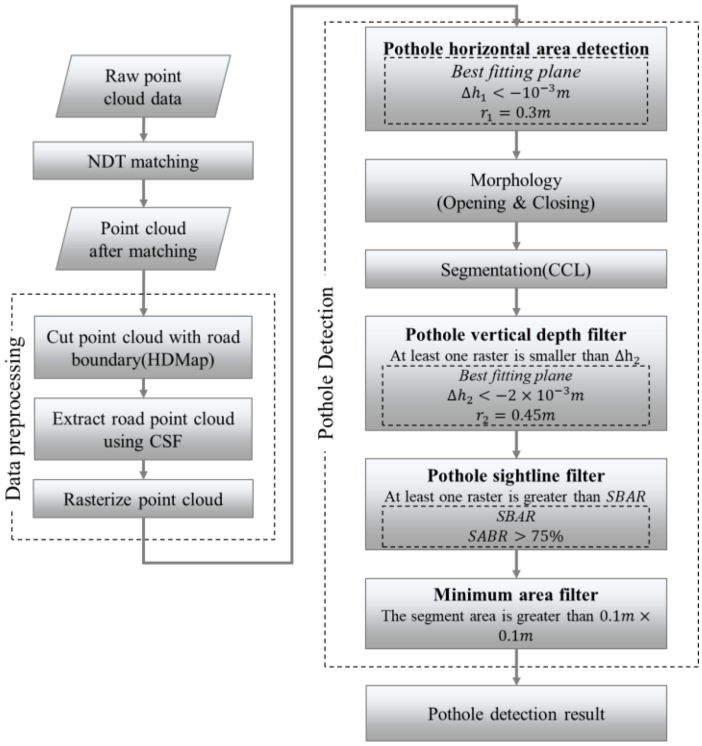

Figure 3. Flow chart of road pavement pothole detection

2.1 Data Preprocessing

Before pothole is detected on 3D point clouds, point cloud matching must be completed. The NDT matching method is performed. Use the point cloud of the HD map (high-definition map) as the base map, and match the point cloud collected by the mobile laser system to the base map. Since HD map are currently only available in specific fields, in this experiment, terrestrial laser (RIEGL VZ-400) point cloud data is used instead of HD map point cloud data as the base map for NDT matching. In data preprocessing, firstly, the point cloud must be cut through the road boundary vector layer of the HD map. The point cloud within the road range must be preserved. The absolute accuracy of the HD map vector layer is 30 cm, and the relative accuracy is 20 cm. Then, through the Cloth Simulation Filter (CSF) algorithm, the ground points within the road boundary are calculated, and the required road point cloud is extracted. Once the extraction is done, a 2D grid map that covers the point distribution area on the XY plane is generated. After the above steps are completed, the data preprocessing is over.

2.2 Pothole Detection

In the process of pothole detection, the pothole horizontal area detection is firstly carried out and calculated by the best fitting plane method. The center of each grid is defined as a searching point with elevation value interpolated from nearby point cloud using IDW (Inverse Distance Weight) method. The search radius is set to 0.3 meters. A plane was fitted to the point cloud within radius from the searching position. The best fitting plane algorithm is shown in Figure 4. If the estimated searching point elevation is lower than the fitted plane and the elevation difference (Δh_1) is larger than 0.001m, the raster in where the searching point locates is considered as a pothole candidate (Figure 6a). For the analysis of the pothole horizontal area detection parameters, please refer to Chapter 4.1. After obtaining the pothole candidate raster, 2D grid map is under morphological process to remove noise (Figure 6b), then CCL (Connected Component Labeling) is implemented to integrate neighboring candidates into one segment. Lastly, pothole segments are processed by three filters, one is pothole vertical depth filter, another is pothole sightline filter, and the other is minimum area filter. Pothole vertical depth filter checks on the elevation difference (Δh_2) between each searching point and its corresponding fitted plane. Segments contain at least one raster possess elevation difference larger than 0.002m are considered as potential potholes, and so are remained (Figure 6c). For the analysis of the pothole vertical depth detection parameters, please refer to Chapter 4.2. Pothole sightline filter use sightline blocked azimuth ratio (SBAR) algorithm. It calculates the ratio of occlusion caused by nearby raster around each searching point. The raster is considered as an occlusion when its center elevation is higher than the current searching point. The SBAR calculation method is shown in Figure 5. If one of the occlusion ratio of the searching point within a segment is higher than 80%, then the segment is considered as a pothole (Figure 6d). SBAR is mainly used to eliminate the terrain where the road edge suddenly drops. Because the road needs to have drainage measures, the road tends to slope outward. The height difference with the road shoulder causes the ground to drop suddenly and may cause error detection. Using the SBAR algorithm, the edge of the road where only half of sightline is blocked can be eliminated. For the analysis of the pothole sightline detection parameters, please refer to Chapter 4.3. The last is pothole minimum area filtering. Pothole candidate segments must be larger than 0.1m×0.1m. Finally, the pothole detection results are obtained.

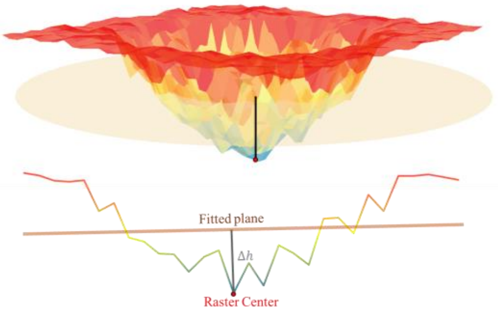

Figure 4. Best fitting plane algorithm

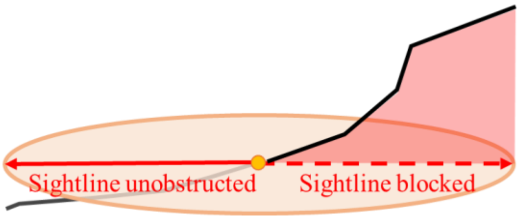

Figure 5. Sightline blocked azimuth ratio algorithm

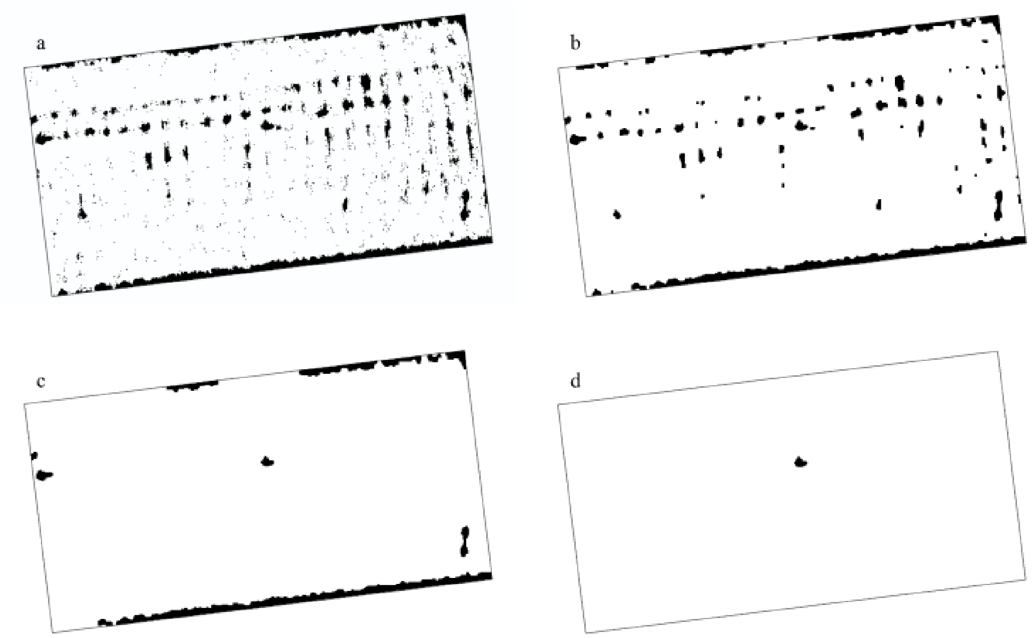

Figure 6. Pothole detection results a. Pothole horizontal area detection result b. Pothole horizontal area detection result after morphology c. Pothole vertical depth detection filter result d. Pothole sightline detection filter result

4. PARAMETERS ANALYSIS

4.1 Pothole Horizontal Area Detection Parameters Analysis

In the detection of the horizontal range of potholes, the parameters to be analyzed are the search radius ($\boldsymbol{r_1}$) and the depth threshold value ($\boldsymbol{\Delta h_1}$), and the goal is to obtain the area closest to the real pothole. Therefore, IOU is used for parameter analysis in the step. The formula of IOU is:

$$\boldsymbol{IOU} = \frac{\boldsymbol{A \cap B}}{\boldsymbol{A \cup B}} \qquad (1)$$

Among them, A is the real value area of the manually digitized pothole in this experiment, and B is the identification area of the pothole detection module. When the shapes of A and B are more similar and overlap, the larger the IOU value is. Referring to the radius size range of general potholes, the search radius is tested from a minimum of 0.05 meters to a maximum of 0.7 meters, and the spacing is 0.05 meters. The depth threshold value is negative at the ground depression, from the shallowest -0.001m to -0.01m, and the interval is 0.001m. It can be seen from Figure 7 that the search radius is 0.3 meters and the depth threshold is -0.001 meters, which has the best median and mean IOU values. Therefore, in this experiment, the search radius ($\boldsymbol{r_1}$) is 0.3 meters and the depth threshold ($\Delta\boldsymbol{h_1}$) is - 0.001 meters are used as the pothole horizontal area detection parameters.

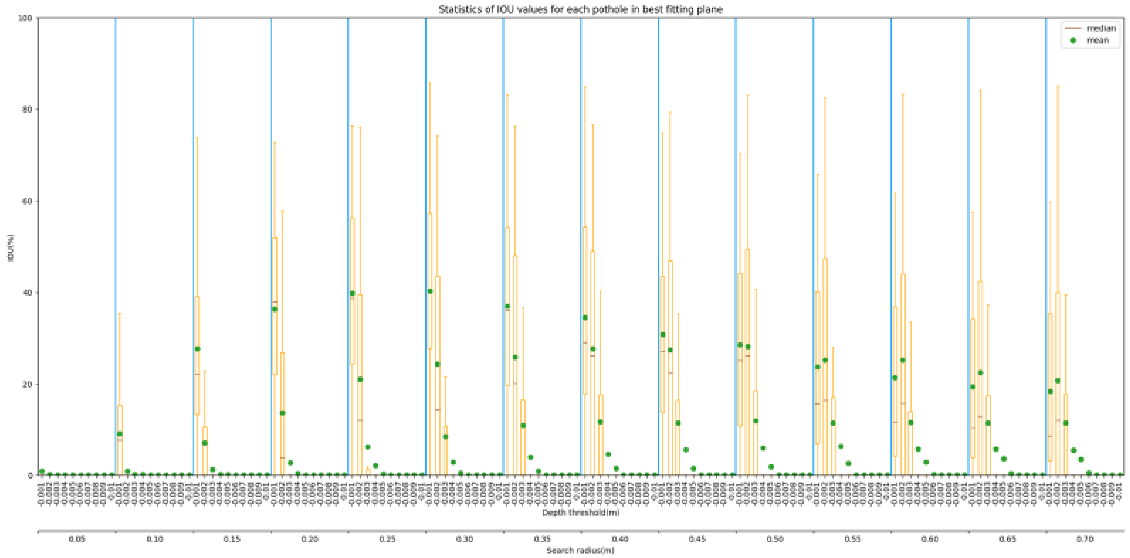

Figure 7. Statistical chart of IOU parameter analysis of pothole horizontal range detection

4.2 Pothole Vertical Depth Filter Parameters Analysis

The pothole vertical depth filter is used to filter shallow and small sinkholes that are not potholes. It is expected to detect the maximum number of real potholes as the premise, and filter out the misjudgment results of non-potholes. This parametric analysis analyzes the search radius ($\boldsymbol{r_2}$) and depth threshold ($\Delta\boldsymbol{h_2}$) using Precision and Recall. The formulas for precision and recall are:

$$\boldsymbol{Precision} = \frac{\boldsymbol{TP}}{\boldsymbol{TP+FP}} \qquad (2)$$

$$\boldsymbol{Recall} = \frac{\boldsymbol{TP}}{\boldsymbol{TP+FN}} \qquad (3)$$

TP is a true positive, which means that the real pothole is correctly detected; FP is a false positive, which means that a false pothole is incorrectly detected, which is regarded as a misjudgment; FN is a false negative, which means that the real pothole has not been detected, and it is regarded as a missed judgment. Figure 8 shows that at maximum recall, a search radius of 0.45 m and a depth threshold of -0.002 m have the best precision values. Therefore, in this experiment, the search radius ($\boldsymbol{r_2}$) of 0.45 meters and the depth threshold ($\Delta\boldsymbol{h_2}$) of -0.002 meters are used as the pothole vertical depth filter parameters.

Figure 8. Statistical chart of precision and recall parameter analysis of pothole vertical depth filter

4.3 Pothole Sightline Filter Parameters Analysis

Pothole sightline filter is also analyzed using precision and recall, with the aim of eliminating terrain where the edge of the pavement drops abruptly. Figure 9 shows the pothole detection precision rate and recall rate of each SBAR threshold value. Considering the comprehensive performance of the two, 80% is finally selected as the SBAR threshold value.

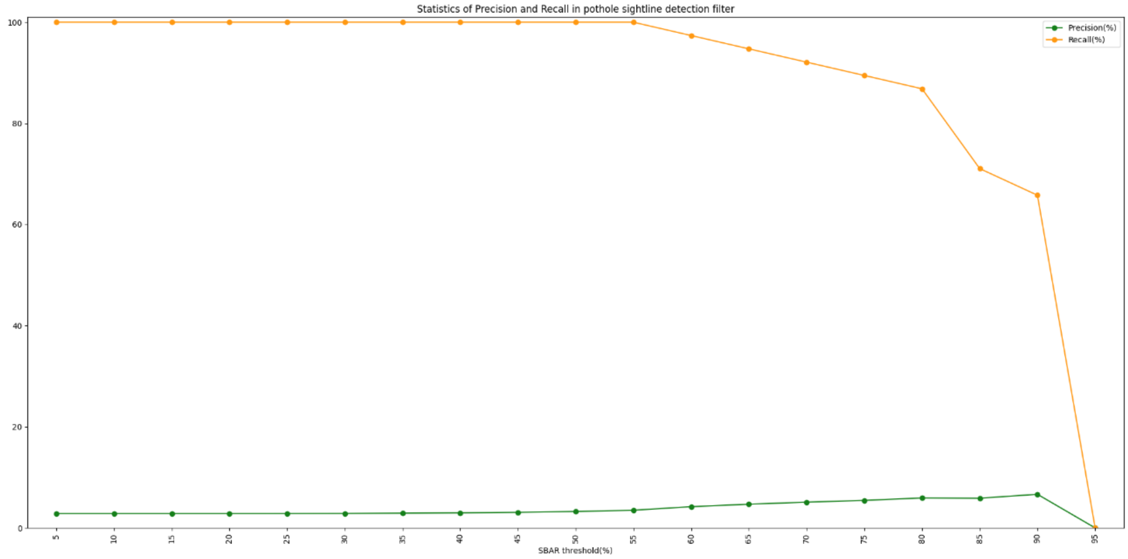

Figure 9. Statistical chart of precision and recall parameter analysis of pothole sightline filter

5. RESULT

Table 1 shows the statistical results of this study. A total of 41 potholes were collected in this experiment. By manually digitizing the area of potholes on the point cloud as the true value, compare the results of the pothole detection module, and analyze the results based on the number of potholes. The number of successfully detected potholes is 34, the misjudged potholes is 686, the missed potholes is 7, the precision is 4.72%, and the recall is 82.93%. Figure 10 shows the first example of pothole detection results. From the experimental results, it can be found that the method used in this paper can indeed perform pothole detection. However, due to the difficulty of matching the 64-line LiDAR in the NDT matching, the road pavement elevation variation is large, which in turn affects the pothole detection module in areas with large elevation variation. This misjudgment can be seen from the second example of pothole detection results in Figure 11.

Real number of potholes	TP	FP	FN	Precision(%)	Recall(%)
41	34	686	7	4.72	82.93

Table 1. Pothole detection results statistics table

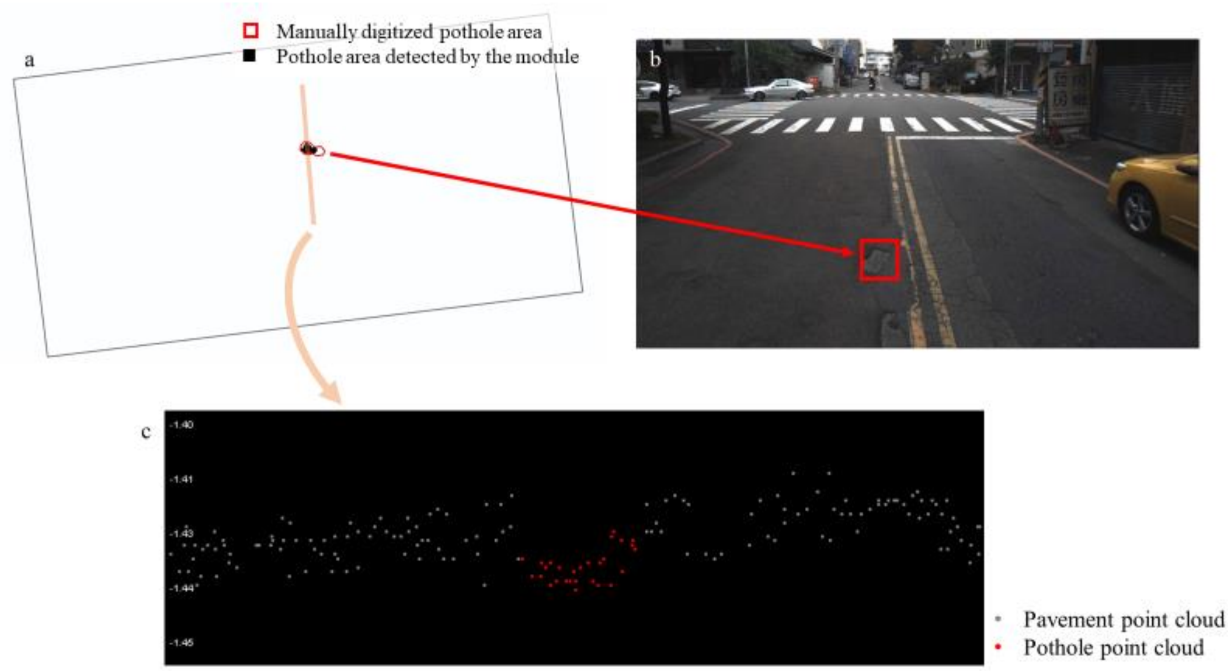

Figure 10. Pothole detection results example 1 a. Pothole area detected by the module and manual digitized pothole area b. Pothole image c. Profile of pothole detection results

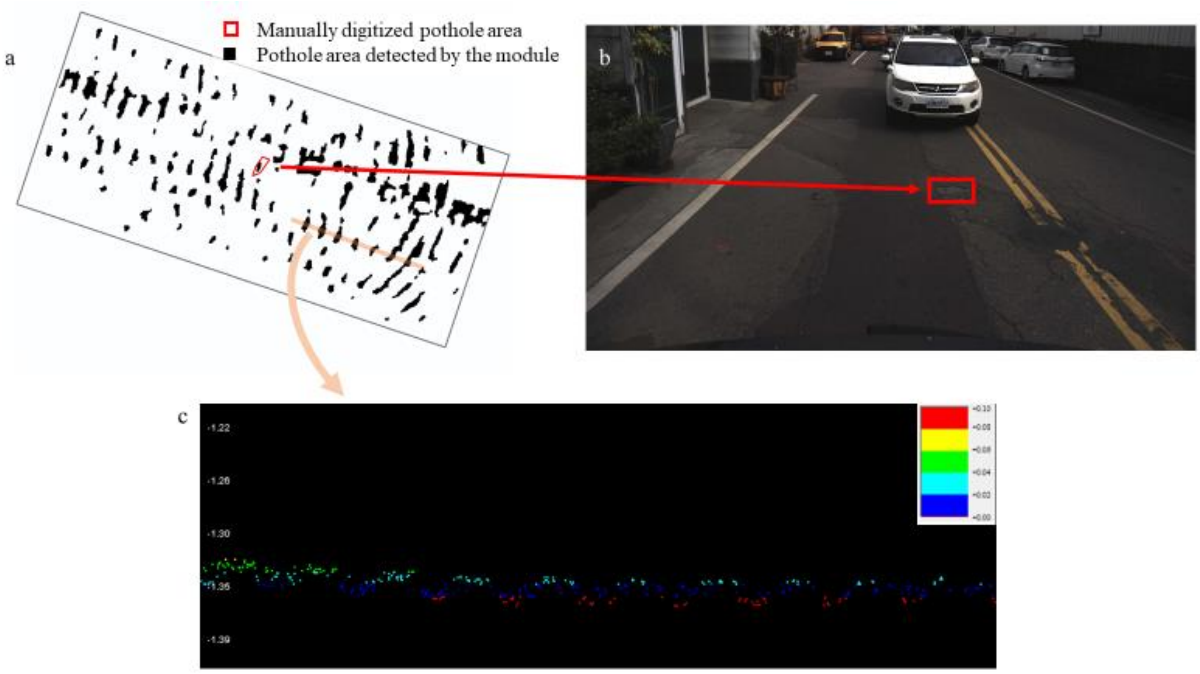

Figure 11. Pothole detection results example 2 a. Pothole area detected by the module and manual digitized pothole area b. Pothole image c. Profile of pothole detection results

6. CONCLUSION

This experiment currently uses 64-line LiDAR point cloud data. The HD map point cloud is used to assist point cloud matching, and potholes can be detected. However, it is difficult to matching in the NDT matching, so that the point cloud contains a large amount of elevation variation, which affects the accuracy of pothole module detection. The problem of point cloud matching will be improved in the future. In addition, this experiment will continue to analyze the threshold value of the best fitting plane algorithm and the sightline blocking azimuth angle ratio, hoping to obtain a better pothole detection precision with the most suitable threshold value.

7. REFERENCES

Kim, T., & Ryu, S. K. (2014). Review and analysis of pothole detection methods. Journal of Emerging Trends in Computing and Information Sciences, 5(8), 603-608.

De Blasiis, M. R., Di Benedetto, A., & Fiani, M. (2020). Mobile laser scanning data for the evaluation of pavement surface distress. Remote Sensing, 12(6), 942

Ravi, R., Habib, A., & Bullock, D. (2020). Pothole Mapping and Patching Quantity Estimates using LiDAR-Based Mobile Mapping Systems. Transportation Research Record, 2674(9), 124-134

Ravi, R., Bullock, D., & Habib, A. (2020). Highway and Airport Runway Pavement Inspection Using Mobile LiDAR. The International Archives of Photogrammetry, Remote Sensing and Spatial Information Sciences, 43, 349-354.